Springer

KSME

Journal of Mechanical Science and Technology 29 (12) (2015) 5437~5446
www.springerlink.com/content/1738-494x(Print)/1976-3824(Online)
DOI 10.1007/s12206-015-1145-3

A modified perturbation/correlation method for force-guided assembly †

Jaesung Oh and Jun-Ho Oh*

Department of Mechanical Engineering, Korea Advanced Institute of Sci. & Tech., 291 Daehak-ro, Yuseong-gu, Daejeon, 305-701, Korea

(Manuscript Received April 3, 2015; Revised July 14, 2015; Accepted August 13, 2015)

Abstract

The present study proposes the Modified perturbation/correlation method (MPCM) as a way of performing assembly tasks and an algorithm by which assembly task can be performed automatically, without human intervention. The MPCM is a method where position/orientation perturbation is generated when the female connector and the male connector are connected and the correlation value of the resulting reaction force/moment is used to calculate and to correct the position and orientation errors between the connectors. The successful performance of assembly task within a limited error range can be confirmed by applying the MPCM to DRC-HUBO. When there are errors between the connector, the correlation value can be confirmed to converge to 0 as errors are corrected even though it takes on certain directionality.

Keywords: Perturbation method; Force-guided assembly; Peg-in-hole task; DRC; DRC-HUBO

1. Introduction

The DARPA Robotics Challenge (DRC), hosted by the Defense Advanced Research Project Agency (DARPA) in the United States in 2013, was a competition to select the robots best able to perform diverse tasks in disaster environments in place of humans, using instruments used by humans. In the DRC, the contestants had to perform a total of eight tasks including driving vehicles, removing obstacles, opening doors, climbing ladders, drilling wall, closing valves, and assembling fire hoses.

To perform the tasks above perfectly, the robot had to be able to judge their respective conditions and the external environment arbitrarily and to interact with the external environment. Most of the robot used vision systems to recognize external environments. Indeed, all teams participating in the DRC sought to resolve the given tasks based on visual information.

However, many teams experienced difficulty in performing the tasks because the current vision systems are imperfect. During the hose assembly task, the existence of the position and orientation error between the female connector and the male connector made it impossible successfully to perform the task. Consequently, although many teams succeeded in holding the female connector with the use of the end-effector of the robot and reaching the male connector, all but two failed to align the connectors and to close the hose [1].

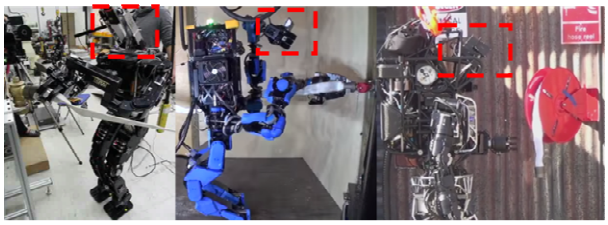

Fig. 1. Hose assembly task using a vision system in DRC trials (DRC-HUBO, SCHAFT, and ATLAS).

Unlike robot, humans can perform assembly task perfectly regardless of the position and orientation errors when to perform the hose assembly task. This is because humans make use of not only visual information but also strength information and the flexibility of the wrist in performing assembly task. Consequently, to perform assembly task successfully it is necessary for a robot to simulate humans' methods.

In studies on assembly task that connect the male connector and the female connector, the field with the most active research is that of peg-in-hole tasks. Peg-in-hole task signify tasks where pegs are literally inserted into holes, and many studies were conducted in this field during the development of industrial robot in the 1980s and 1990s. In fact, numerous methods were proposed as strategies for performing peg-in-hole task.

As solutions to the problem of peg-in-hole task, there are generally three methods that can be applied [2]. The first is to correct the position and orientation error by using vision sys-

*Corresponding author. Tel.: +82 42 350 3263, Fax.: +82 42 350 8900
E-mail address: jhoh8@kaist.ac.kr
† Recommended by Associate Editor Kyoungchul Kong

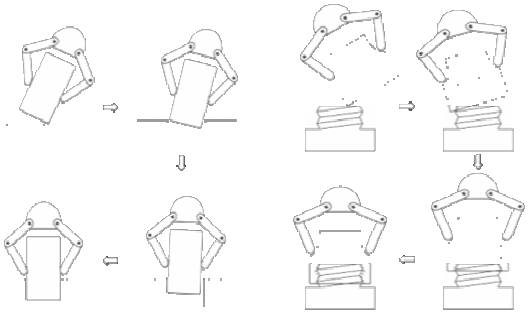

Fig. 2. Process of a peg-in-hole task and a hose assembly task.

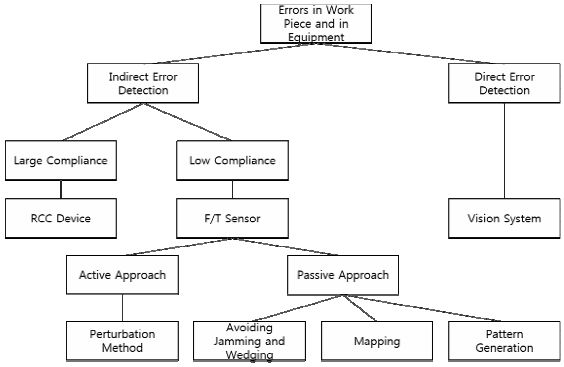

Fig. 3. Strategy for solving a peg-in-hole task.

tems, and visual information obtained from cameras and laser sensors is used [3-5]. The second is to make use of Remote center compliance (RCC) devices, and the flexibility of RCC is used [6-9]. The third is to make use of force-torque sensors (F/T sensor), and force and moment information according to the situation is used [10-26].

However, methods that make use of vision systems are sensitive to external environments and additional error to the recognition of objects can occur due to calibration error. Because methods that use RCC devices must substitute end-effector with RCC devices, they are not easy to use in cases where diverse tasks must be performed simultaneously.

Consequently, the present study seeks to propose a strategy where assembly task can be performed by focusing on peg-in-hole task strategies that make use of F/T sensor.

2. Relative research

Peg-in-hole task strategies that make use of F/T sensors can largely be classified into four types.

2.1 Avoiding jamming and wedging

By using a 3DOF (F_z, M_x, M_y) F/T sensor and Selective Compliance Assembly Robot Arm (SCARA), Puente judged an approach to be successful when the F_z value reached a certain amount. Then the presence of jamming and wedging was judged according to the sizes and signs of moment_x and moment_y. As the direction for avoiding them, position error was corrected while changing the position of the peg [10]. Jamming signifies a state where, when inserting the peg in the hole, the peg can no longer enter the hole and stops due to the friction generated as the peg comes in contact with the surface of the hole. Wedging signifies a state where, due to the influence of the reaction force and friction generated on the surface, the peg is completely stuck in the hole. In the case of jamming, the state can be undone when the direction in which force is applied is changed to reduce friction. In the case of wedging, however, the state cannot be undone even when the direction in which force is applied is changed because both friction and reaction force are at work.

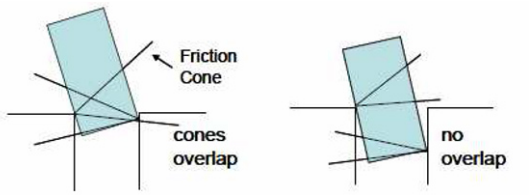

Fig. 4. Wedging and jamming configuration.

Using a 3DOF F/T sensor, Sathirakul divided the contact state of the task of inserting a dual peg into a total of thirteen stages, and generated a jamming diagram for each case, thereby seeking to resolve the problem of jamming that can occur while performing peg-in-hole task [11]. Developing this, Xia studied strategies for performing peg-in-hole task and avoiding the problem of jamming by using a 6DOF F/T sensor to divide cases into those not touching the contact state, touching it at one point, and touching it at two points and establishing 3D jamming space [12]. DiCicco sought to solve the problem of jamming by measuring the force and the moment of each axis with a 6DOF F/T sensor, calculating the friction due to the state of the contact, calculating a jamming matrix, and ensuring that friction did not exceed the force entered [13]. The strategy to use jamming diagrams or jamming matrices to resolve peg-in-hole task has the advantage of being able to judge jamming or wedging. However, it has the disadvantage of not being able to present the direction for correcting the positions of the peg and the hole and orientation error.

2.2 Mapping and inverse mapping

Chhatpar suggested a peg-in-hole task strategy that made use of a tilt strategy. Since the amount of tilt generated changes with the application of certain pressure in accordance with the relative positions of the peg and the hole, mapping was performed by using the tilt value, which changes according to the position [14]. Taking a hint from a study by Inoue and Simunovic, this used the changing degree of the tilt generated when pushed with pressure, in accordance with the relative positions of the hole and the peg [15, 16]. Newman created a map by measuring the force and the moment when the peg and the hole reached a static equilibrium [17]. Here, to obtain

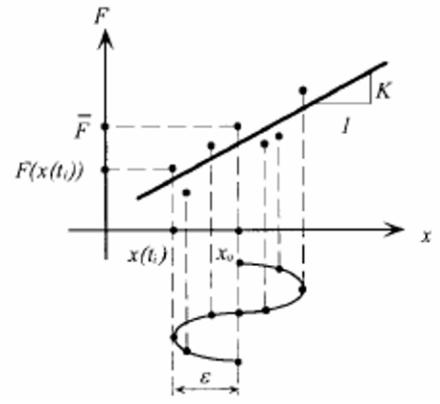

Fig. 5. Perturbation method and linear regression.

ideal data, the influence of friction and dynamics was offset by using a controller. In addition, to create unique mapping between the position and the force/moment, the force and the moment were measured when the position changed subtly. Subsequent data were gathered in a single cluster, a K-mean algorithm was applied, and, through this, only valid data were used to create a map [18].

Using the method above, Dietrich created a force/torque map and a redundancy map. In addition, by creating maps for cases where not only the position but also the orientation differed, lookup tables for diverse cases were created to perform peg-in-hole task [19]. Because the method, using mapping and backward mapping, possesses force and moment information according to the position, it can promptly provide information on the next position. However, it has the disadvantage that a considerable number of repetitions are necessary before performing tasks, and that a map must be newly created for each changed condition.

2.3 Pattern generation

A recent trend in research on peg-in-hole task is to use patterns, and this method is more intuitive than existing ones. Chen proposed a method where peg-in-hole task was divided into the three stages of searching, insertion, and settle-down. A circular position pattern with a gradually increasing radius was established in the searching state, and the position of the hole into which the cylindrical peg is to be inserted was discovered by using the changing force/T sensor value during the progress of the pattern [20]. By using a non-cylindrical peg and adding an orientation pattern to the position pattern, Park proposed a peg-in-hole task strategy that was prompt and intuitive regardless of the shape vertical to the interface [21]. By using patterns, it is possible to perform peg-in-hole task very promptly and accurately when only position error exists. However, there is the disadvantage that it is very difficult to take orientation error into consideration and to avoid jamming or wedging when it occurs, and that the system can be damaged.

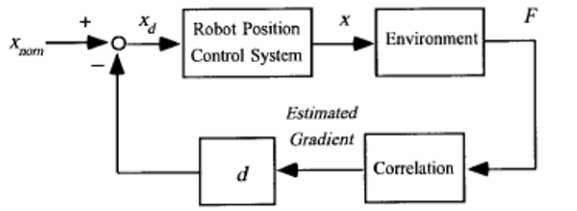

Fig. 6. Block diagram of the control system of PCM.

2.4 Perturbation method

To overcome the shortcoming above, Lee proposed the Perturbation/correlation method (PCM) [22-24]. The PCM is a method where, with the peg and the hole in contact with each other, position perturbation is generated and the correlation values of the ensuing reaction force and position perturbation are used. Here, correlation has the characteristic of presenting the direction for minimizing the performance index. When the least square method is used, it is possible to see the relationship between the gradient and the correlation mathematically.

$$
\begin{aligned}
&p(t) = p_0 + \varepsilon\delta_p(t)\\
&\delta_p(t) = \sin(\omega_p t)\\
&R_p = \int_t^{t+\frac{2\pi}{\omega_p}} \delta_p(\tau)F(p(\tau))d\tau = \sum_{i=1}^{2n} F(t_i)\varepsilon\sin\left(\frac{\pi}{n}i\right)\\
&t_i = \frac{\pi i}{n\omega_p},\ \ i = 1, 2, ..., 2n\\
&\bar{p} = \frac{1}{2n}\sum_{1}^{2n} p(t_i) = \overline{p_0}\\
&\bar{F} = \frac{1}{2n}\sum_{1}^{2n} F(t_i)\\
&\frac{\partial F}{\partial x} = K = \frac{\sum_{i=1}^{2n}\left[p(t_i)-\bar{p}\right]\left[F(t_i)-\bar{F}\right]}{\sum_{i=1}^{2n}\left[p(t_i)-\bar{p}\right]^2}\\
&K = \frac{\sum_{i=1}^{2n} F(t_i)\varepsilon\sin\left(\frac{\pi}{n}i\right)}{n\varepsilon^2} = \frac{R_p}{n\varepsilon^2}.
\end{aligned}
\tag{1}
$$

Lee's method has the advantage of relatively reducing the occurrence probability of jamming due to continuous perturbation and correcting the position error of peg and hole without prior execution [25, 26]. However, it has the disadvantage of not being able to correct orientation error and to take into consideration the time delay generated between the input (perturbation) and the output (measured force).

Because it is possible to establish the peg and the hole in peg-in-hole task as the male connector and the female connector in assembly task, respectively, this paper proposes a new Modified perturbation/correlation method (MPCM) to per-

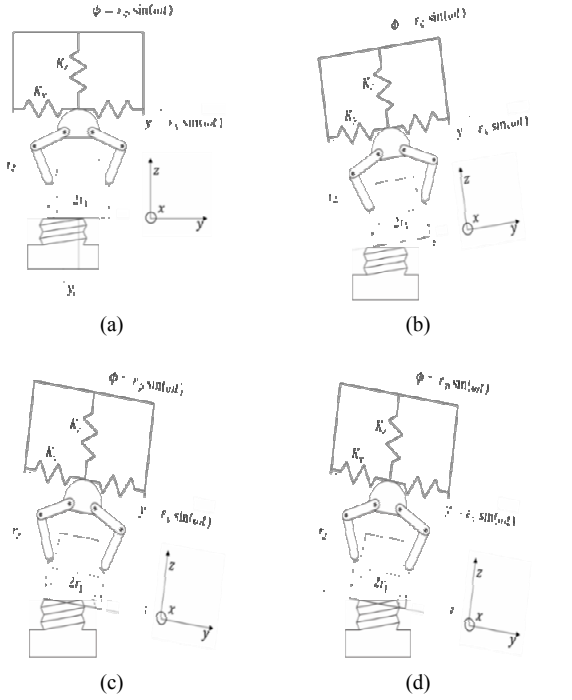

Fig. 7. (a) Case a: configuration of a positive position error without an orientation error; (b) case b: configuration of a positive orientation error with a positive position error; (c) case c: configuration of a negative orientation error with a positive position error with a top contact; (d) case d: configuration of a negative orientation error with a positive position error with a side contact.

form assembly task by supplementing the PCM proposed as a strategy for peg-in-hole task.

3. Modified perturbation/correlation method (MPCM)

Because the PCM proposed by Lee makes use of the correlation between the input (position perturbation) and the output (reaction force and moment), the time delay needed for the system process must be taken into consideration. Consequently, sufficiently slow perturbation must be used so that the correlation value is not changed considerably due to time delay. In addition, because only the position error of the male connector and the female connector are taken into consideration, and the information on orientation error is not taken into consideration at all, only very limited assembly task can be performed.

Consequently, the present study proposes the MPCM. The MPCM makes use of not only position perturbation but also orientation perturbation. By using the correlation between the reaction force and the moment generated according to perturbation when the position and orientation error exist, it presents the direction of the position and the orientation that can minimize the performance index R (correlation of reaction force and moment). Because the MPCM makes use of the correlation between the results of movement, there is no need to take into consideration the time delay generated by the system process, and it possible to use perturbation at a very high speed and to reduce the time needed for assembly task efficiently.

3.1 Mathematical modeling

Depending on the contact state of the male and female connector, the reaction force and the moment of perturbation differ. To calculate the reaction force and the moment arising from perturbation mathematically, the following is hypothesized: the amplitude of perturbation is very small and all movements are quasi-static.

The biped robot platform is used for experiments, and it can be unstable due to a large external force which is made by perturbation. Therefore, that assumption is must necessary, and the amplitude and speed of the perturbation that is used for MPCM is experimentally determined.

A total of four contact states can occur during the performance of assembly task. Even cases where the axes correspond to each other and differ from each other are considered to be identical.

Performance index R and constraints of contact force condition or maximum error are determined when input is orientation and position perturbation.

Eqs. (2) and (3) show the process for calculating performance index R under condition of case a in Fig. 7(a)

$$
\begin{aligned}
&\phi = \varepsilon_{\phi}\sin(\omega t)\\
&\text{If } \ 0 < t < \frac{\pi}{2\omega}\\
&F_z = \overline{F_z} + K_z r_1 \sin(\phi)\\
&M_x = \overline{M_x} - \mu N r_2 - K_y r_1 r_2\left(1-\cos(\phi)\right) - K_z r_1^2 \sin(\phi)\\
&N = F_z\\
&\text{If } \ \frac{\pi}{\omega} < t < \frac{3\pi}{2\omega} \qquad (2)\\
&F_z = \overline{F_z} - K_z\left(r_1 - y_e\right)\sin(\phi)\\
&M_x = \overline{M_x} + \mu N r_2 + K_y\left(r_1 - y_e\right) r_2\left(1-\cos(\phi)\right)\\
&\qquad - K_z\left(r_1 - y_e\right)^2 \sin(\phi)\\
&R_{x_{ori}} = \int_0^{\frac{\pi}{2\omega}}\left(F_z - \overline{F_z}\right)\left(M_x - \overline{M_x}\right)dt + \int_{\frac{\pi}{\omega}}^{\frac{3\pi}{2\omega}}\left(F_z - \overline{F_z}\right)\left(M_x - \overline{M_x}\right)dt \qquad (3)\\
&K_{yp} = R_{x_{ori}} = -\alpha_1 y_e\\
&y = \varepsilon_y \sin(\omega t)\\
&K_{xo} = \int_0^{\frac{\pi}{2\omega}}\left(F_z - \overline{F_z}\right)\left(M_x - \overline{M_x}\right)dt + \int_{\frac{\pi}{\omega}}^{\frac{3\pi}{2\omega}}\left(F_z - \overline{F_z}\right)\left(M_x - \overline{M_x}\right)dt\\
&K_{xo} = R_{y_{pos}} = \alpha_4 \tan(\phi_e).
\end{aligned}
$$

Eq. (4) is also range of the contact force condition and maximum error under condition of case a

Table 1. Performance index R in accordance with cases a-d.

	Performance index R ($K_{yp} = R_{x_{ori}}$, $K_{xo} = R_{y_{pos}}$)	
	Orientation Perturbation	Position Perturbation
Case a	$-\alpha_1 y_e$	0
Case b	$-\alpha_3$	$\alpha_4 \tan(\phi_e)$
Case c	$-\alpha_5$	$-\alpha_6 \tan(\phi_e)$
Case d	$-\alpha_7$	$-\alpha_8 \tan(\phi_e)$

$$\overline{F_z} - K_z r_1 \varepsilon_\phi > 0$$
$$r_1 - y_e > 0 . \tag{4}$$

Consequently, when the contact force conditions are satisfied, the correlation value of the force/moment according to orientation perturbation is expressed as a function of position error in the case that position error exists, and the correlation value of the force/moment according to position perturbation is expressed as a function of orientation error in the case that orientation error exists. In other words, the correlation value can be used to confirm the sizes and directions of the position and orientation error and to correct the position and the orientation in the direction of reducing error.

$$\alpha_1 = \frac{K_z \mu \overline{F_z} r_2 \varepsilon_\phi}{\omega}$$
$$\alpha_3 = \frac{2}{\omega} K_z r_1 \varepsilon_\phi \mu \overline{N_1} \left(\sqrt{r_1^2 + r_2^2} \cos(\phi_e - \psi_3) \right)$$
$$\alpha_4 = \frac{2}{\omega} K_z \varepsilon_y \mu \overline{N_1} \left(\sqrt{r_1^2 + r_2^2} \cos(\phi_e - \psi_3) \right)$$
$$\alpha_5 = \frac{2}{\omega} K_z r_1 \varepsilon_\phi \mu \overline{N_1} \left(\sqrt{r_1^2 + r_2^2} \cos(\phi_e + \psi_5) \right)$$
$$\alpha_6 = \frac{2}{\omega} K_z \varepsilon_y \tan(\phi_e) \mu \overline{N_1} \left(\sqrt{r_1^2 + r_2^2} \cos(\phi_e + \psi_5) \right)$$
$$\alpha_7 = \frac{2}{\omega} K_z r_1 \varepsilon_\phi \mu \overline{N_2} \left(\sqrt{r_1^2 + r_2^2} \cos(\phi_e + \psi_7) \right) \tag{5}$$
$$\alpha_8 = \frac{2}{\omega} K_z \varepsilon_y \tan(\phi_e) \mu \overline{N_2} \left(\sqrt{r_1^2 + r_2^2} \cos(\phi_e + \psi_7) \right)$$
$$\psi_3 = \cos^{-1} \left(\frac{r_2}{\sqrt{r_1^2 + r_2^2}} \right)$$
$$\psi_5 = \cos^{-1} \left(\frac{r_2}{\sqrt{r_1^2 + r_2^2}} \right)$$
$$\psi_7 = \cos^{-1} \left(\frac{r_1}{\sqrt{r_1^2 + r_2^2}} \right)$$
$$\overline{N_1} = \overline{F_z} \cos(\phi_e) + \overline{F_y} \sin(\phi_e)$$
$$\overline{N_2} = \overline{F_z} \sin(\phi_e) + \overline{F_y} \cos(\phi_e) .$$

To maintain the connected state, the contact force must always have a positive value. In addition, when the signs of error are identical, for them to have the signs of correlation, the following contact force conditions must be satisfied.

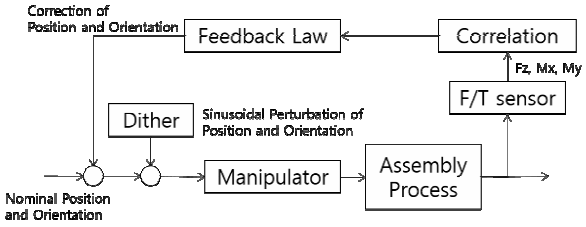

Fig. 8. System diagram of MPCM.

$$\overline{F_z} > K_z r_1 \varepsilon_\phi$$
$$\overline{F_z} > K_z \varepsilon_y \tan(\phi_{e,limit})$$
$$\overline{F_z} < \frac{\rho_1 + K_z \varepsilon_y \tan(\phi_e) \sin(\phi_e) + K_y \varepsilon_y \cos(\phi_e)}{\sin(\phi_e)}$$
$$\overline{F_z} < \frac{\rho_2 - K_z r_1 \varepsilon_\phi \sin(\phi_e)}{\sin(\phi_e)}$$
$$\overline{F_y} > K_y \varepsilon_y \tag{6}$$
$$\overline{F_y} > \frac{\rho_1 + K_z \varepsilon_y \tan(\phi_e) \sin(\phi_e) + K_y \varepsilon_y \cos(\phi_e) - \overline{F_z} \sin(\phi_e)}{\cos(\phi_e)}$$
$$\overline{F_y} > \frac{\rho_2 - K_z r_1 \varepsilon_\phi \sin(\phi_e) - \overline{F_z} \sin(\phi_e)}{\cos(\phi_e)}$$
$$\rho_1 = \frac{K_y \varepsilon_y r_2 + K_z \varepsilon_y \tan(\phi_e) r_1}{\mu \cos(\phi_e + \psi_8) \sqrt{r_1^2 + r_2^2}}$$
$$\rho_2 = \frac{K_z r_1^2 \varepsilon_\phi}{\mu \cos(\phi_e + \psi_7) \sqrt{r_1^2 + r_2^2}} .$$

3.2 System diagram

The positions of the state in which the female and male connector are connected are established as the nominal position and orientation. Here, position and orientation perturbation are generated independently, and the correlation between the reaction force and the moment with respect to movements is calculated. It is called performance index to reduce the position and orientation errors. By using the correlation calculated and applying it to the feedback law, the nominal position and the orientation are modified.

3.3 Feedback law

Because the correlation value possesses the size and the direction capable of correcting the position and orientation error, it can be used as feedback gain by multiplying it with a certain constant.

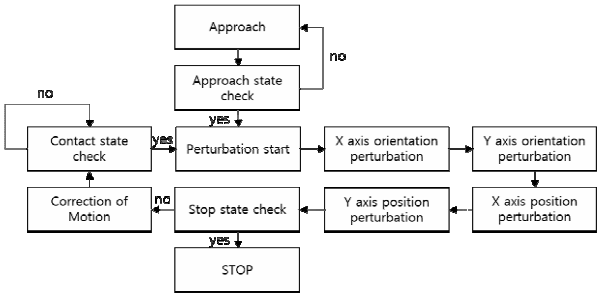

Fig. 9. Algorithm that can automatically perform an assembly task using MPCM.

$$\frac{\Delta x_d}{T} = -\beta_1 K_{xp}$$
$$\frac{\Delta y_d}{T} = -\beta_2 K_{yp} \quad (7)$$
$$\frac{\Delta \phi_d}{T} = -\beta_3 K_{xo}$$
$$\frac{\Delta \theta_d}{T} = -\beta_4 K_{yo} .$$

Consequently, the nominal coordinates of the end-effector can be corrected as follows to correct the position and orientation error between the connector.

$$x_d = x_n - \beta_1 \Sigma K_{xp}$$
$$y_d = y_n - \beta_2 \Sigma K_{yp}$$
$$\phi_d = \phi_n - \beta_3 \Sigma K_{xo} \quad (8)$$
$$\theta_d = \theta_n - \beta_4 \Sigma K_{yo}$$
$$z_d = z_n - \beta_5 (F_{th} - F_z) .$$

Relocating the position in the direction of the z-axis is done to maintain contact state between the connector and ultimately plays the role of inserting the male connector instead of the female connector.

3.4 Assembly process

Because the positions of the x-axis and the y-axis and orientation error must be corrected, a total of four sessions of perturbation and the process of correcting the error of the end-effector by using the correlation values calculated through perturbation are necessary. The contact conditions and stopping conditions are repeatedly judged to proceed with the entire process.

When the force in the direction of the z-axis exceeds a certain threshold value for certain duration, the male and female connector are judged to have been connected and the perturbation stage is implemented. In the present study, the threshold force and the judgment time are established as 3 N and 0.1 s, respectively.

In the process of correcting error according to perturbation, the correlation between the force and the moment becomes 0 at some point. However, because it is impossible to precisely maintain the value of 0, the sign of the correlation value repeatedly alternates between positive and negative numbers. Consequently, when the sign of correlation continues to change for a certain number of times, the alignment between connector is judged to be proper and perturbation is stopped. In the present study, perturbation was stopped after a sign change occurred four or more times.

To obtain the desired correlation values through the subsequent perturbation after correcting error, the contact force and the moment must be adjusted to the set values. Consequently, when the contact force and the moment do not satisfy the set values after error has been corrected, the established contact force and moment must be satisfied by relocating the x, y, and z position of the end-effector.

Fig. 10. Humanoid platform, DRC-HUBO.

4. Experimental setup for hose assembly task

As the humanoid platform for the experiments, DRC-HUBO was used. Because the base of most industrial robot is fixed on a high-weight surface plate, unstable posture due to external force need not be taken into consideration. However, because a humanoid robot maintains a state of standing on two feet on the ground, the posture can easily become unstable even with small external force.

To apply the MPCM to humanoid robot, a posture that can withstand the external force must be assumed and the reaction force/moment must be established to be as small as possible. In addition, the speed and amplitude of perturbation must be reduced and, by doing so, the generation of external force by perturbation must be minimized as much as possible.

A humanoid robot stands with its legs apart in the stop state. Here, because the support surface is longer laterally than longitudinally, robot can better withstand external force acting on the front and back than an external force acting left and right.

Table 2. Manipulability comparison in accordance with the humanoid robot posture.

	Frontal	Lateral
Configuration	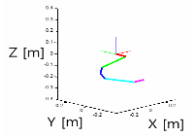	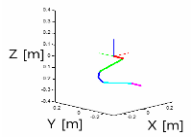
	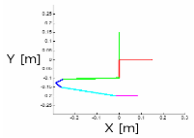	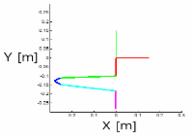
Manipulability	11.7659	112.2432

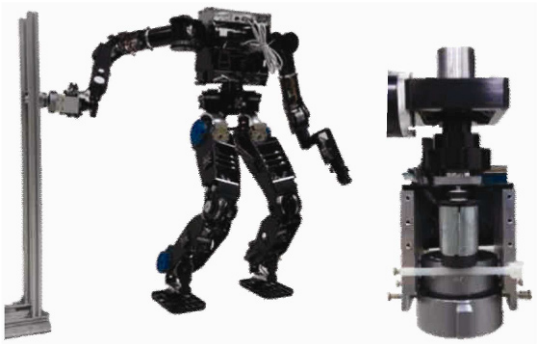

Fig. 11. Humanoid robot posture for performing an assembly task and a humanoid hand is replaced to a female hose connector.

Consequently, to secure sturdiness with respect to external force, the knees must be bent and the legs must be spread to lower the center of mass and to broaden the support polygon.

In addition, manipulability can be confirmed to be higher when the assembly task posture is lateral than when it is longitudinal.

The end-effector of DRC-HUBO is mounted with a hand consisting of three fingers. However, to apply the MPCM, the coordinate of the F/T sensor and the coordinate of the female connector must be identical, which makes it difficult to perform assembly task while holding the female connector with the hand. Consequently, the MPCM is implemented after substituting the humanoid hand with the female connector, as follows.

Normally, raw F/T sensor signals have a high frequency noise, so they cannot be directly used for analysis. Therefore, the 1st LPF, which has a cut-off frequency as the frequency of perturbation, is used to reduce the high frequency noise of raw F/T sensor signals.

5. Experimental result using MPCM

5.1 Position/orientation error limit and condition of contact force/moment

To determine the actual position/orientation error restrictions and the contact force/moment conditions, the spring constant must be obtained. The spring constant is measured by fixing the end-effector of the robot and measuring the force and the moment according to subtle movements in an isometric state.

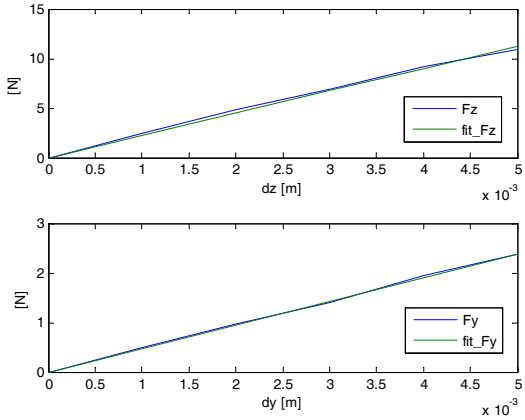

Fig. 12. Calculation of an effective spring constant using measured force and moment, $K_z = 2254.5\ [N/m]$, $K_x = K_y = 466.8\ [N/m]$. Under contact conditions, the reaction force and moment are calculated using effective stiffness. In order to use position control to move the robot, the effective stiffness is related to the manipulation controller gain and stiffness of the external environment, in this case, an aluminum fire hose is used for the experiment.

When the correctable maximum errors which are 0.03 [m] and 10.95 [°] are obtained by using a mathematical model, it is as follows.

$$
\begin{aligned}
& y_e < r_1 = 0.03[\mathrm{m}] \\
& \phi_e < \tan^{-1}\left(\frac{K_y r_2}{K_z r_1}\right) = 47.60[^\circ] \\
& \phi_e < \frac{\pi}{2} + \cos^{-1}\left(\frac{r_2}{\sqrt{r_1^2 + r_2^2}}\right) = 100.95[^\circ] \\
& \phi_e < \frac{\pi}{2} - \cos^{-1}\left(\frac{r_2}{\sqrt{r_1^2 + r_2^2}}\right) = 79.05[^\circ] \\
& \phi_e < \frac{\pi}{2} - \cos^{-1}\left(\frac{r_1}{\sqrt{r_1^2 + r_2^2}}\right) = 10.95[^\circ].
\end{aligned}
\tag{9}
$$

When the amplitude and speed of perturbation are established with the size of orientation being $0.25[^\circ]$, the size of position being $0.5[\mathrm{mm}]$, and the speed as $2[\mathrm{Hz}]$, the contact force/moment conditions can be obtained, as follows. The material of the connector used in the experiments was, and the coefficient of static friction generated between aluminums was 1.

When $\overline{F_z}$ is established, $\overline{F_y}$ can be established too. Here, the range of $\overline{F_y}$ changes according to the maximum correctible error range. In the present experiments, the connected force and the moment and the correctible error range were

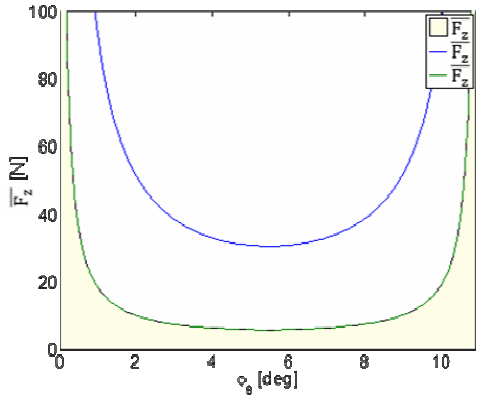

Fig. 13. Condition of z-axis contact force ($\overline{F_z}$). If $\overline{F_z}$ exceed the limited boundary, cases of contact aren't classified using MPCM. $\overline{F_z}$ needs to be preset to determine the range of $\overline{F_y}$ that is expressed as a function of $\overline{F_z}$.

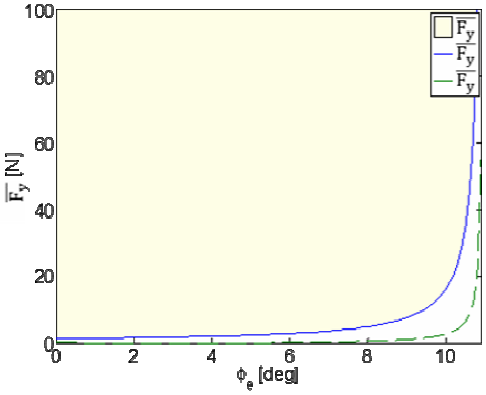

Fig. 14. Condition of the y-axis contact force ($\overline{F_y}$). If $\overline{F_y}$ doesn't exceed the limited boundary, cases of contact aren't classified using MPCM. The range of orientation error is intentionally limited to prevent damage to the robot since the contact force condition is large enough to deal with a large orientation error.

established, as follows.

$$\begin{aligned} &\overline{F_z} = 3\,[\mathrm{N}] \\ &\overline{F_y} = 3\,[\mathrm{N}] \\ &\overline{M_x} = 0.555\,[\mathrm{N}] \\ &y_{e,\mathrm{limit}} = 0.03\,[\mathrm{m}] \\ &\phi_{e,\mathrm{limit}} = 6.1\,[^\circ]\,. \end{aligned} \tag{10}$$

5.2 Measured force and moment according to connector configuration

When the force and the moment generated after imposing perturbation according to the contact state are measured, they can be confirmed to be similar in size and pattern to the force and the moment theoretically calculated by using mathematical modeling. However, because it is difficult to reproduce cases in actual situations where the orientation error is 0, it can be confirmed that, at such times, the correlation values of the force and the moment according to position perturbation are not precisely 0.

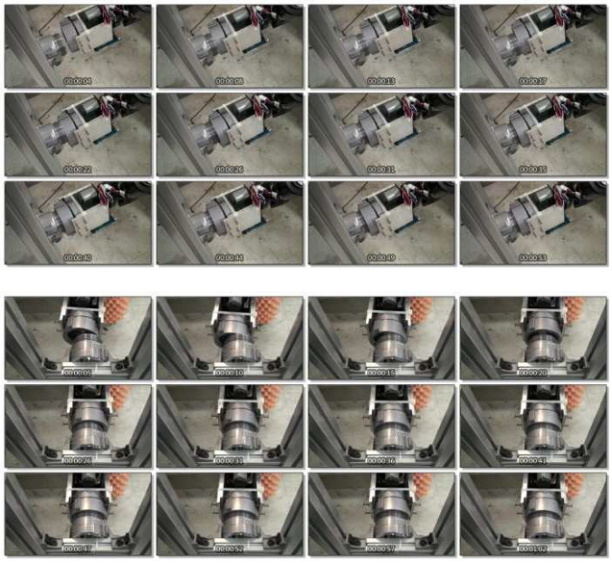

Fig. 15. Hose connector assembly task. The upper snapshot is the side view, and the lower snapshot is the top view. Connectors are automatically aligned using MPCM.

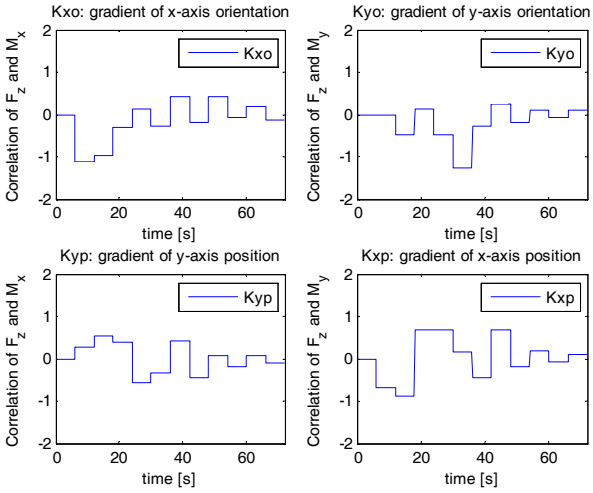

Fig. 16. Correlation of force and moment during the assembly task. The correlation is large when the assembly process starts, but it converges to 0 after a few seconds. That means that two connectors are aligned using MPCM.

5.3 Correlation of force and moment during assembly process

Fig. 15 shows the progress of assembly task when perturbation is established with the amplitude of orientation as 0.25 [°] , the amplitude of position as 0.5 [mm], and the speed as 2 [Hz] and the contact force and the moment are established as $\overline{F_z}$ =3 [N] and $\overline{M_x} = \overline{M_y} = 0.555$ [N], respectively.

With the progress of assembly task, except for cases where

the orientation error is 0, all possible contact states can be confirmed to occur. In addition, the correct direction according to error can be confirmed to progress in the direction of converging error, and this can be confirmed also from Fig. 16. When the male connector and the female connector are properly aligned, it is difficult for error to be precisely 0. Consequently, the correlation values of the force and the moment can be confirmed to manifest themselves repeatedly as positive and negative numbers. By stopping the task when changes in the signs were repeated for a certain number, it was possible to proceed with assembly task without human intervention.

6. Conclusion

This paper proposes the Modified perturbation/correlation method (MPCM) and algorithm to automatically perform assembly task without human intervention. The MPCM is a method where position/orientation perturbation is generated when the female connector and the male connector are connected and performance index R (the correlation value of the resulting reaction force/moment) is used to calculate the position/orientation errors between the connectors. The original PCM method only considers position errors, and it does not consider orientation errors of connectors. The successful performance of assembly task within a limited error range can be confirmed by applying the MPCM to DRC-HUBO. Here, because the posture of the robot could become unstable as the external force increased, it was possible to secure robustness with respect to external force and comparatively high manipulability by spreading the legs of the robot and establishing the initial posture laterally instead of longitudinally.

The present study is limited in that it replaced the end-effector with the female connector to establish the same z-axis for the female connector and the F/T sensor. Indeed, for humanoid robot to perform assembly task, the female connector is taken hold of and tasks are performed. Here, if the x-axis and y-axis position/orientation coordinate of the female connector and the F/T sensor are not identical, offset components arise, thus making it impossible to impose perturbation vertical to the desired female connector and therefore to use the MPCM. Consequently, additional research is necessary so that the MPCM can be applied even when the coordinate of the end-effector and the F/T sensor differ from one another. The biped robot platform can fail due to perturbation which makes the external force and moment have a contact condition with an external environment. Therefore, a stabilizing method is needed to limit the contact force and sustain the ZMP on the support polygon.

References

[1] DRC trials result, http://www.theroboticschallenge.org/.

[2] K. Chang, Physical modeling of tools necessary for robot manipulation, *Doctoral Dissertation*, The University of Texas at Austin (2006).

[3] J. Su, H. Qiao, C. Liu and Z. Ou, A new insertion strategy for a peg in an unfixed hole of the piston rod assembly, *The International Journal of Advanced Manufacturing Technology*, 59 (9-12) (2012) 1211-1225.

[4] S. Molkenstruck, U. Thomas and F. Wahl, Advances in automated robot programming, *3rd International Colloquium of the Collaborative Research Center 562 Braunschweig* (2008) 85-100.

[5] K. Hirana, T. Suzuki, S. Okuma, K. Itabashi and F. Fujiwara, Realization of skill controllers for manipulation of deformable objects based on hybrid automata, *Robotics and Automation*, *Proceedings 2001 ICRA. IEEE International Conference on IEEE*, 3 (2001) 2674-2679.

[6] D. E. Whitney, Quasi-static assembly of compliantly supported rigid parts, *Journal of Dynamic Systems, Measurement, and Control*, 104 (1) (1982) 65-77.

[7] S. Lee, Development of a new variable remote center compliance (VRCC) with modified elastomer shear pad (ESP) for robot assembly, *Automation Science and Engineering, IEEE Transactions on*, 2 (2) (2005) 193-197.

[8] B. Baksys and N. Puodziuniene, Alignment of parts in automatic assembly using vibrations, *Assembly Automation*, 27 (1) (2007) 38-43.

[9] S. Kilikevicius and B. Baksys, Dynamic analysis of vibratory insertion process, *Assembly Automation*, 31 (3) (2011) 275-283.

[10] E. A. Puente, C. Balaguer and A. Barrientos, Force—torque sensor-based strategy for precise assembly using a SCARA robot, *Robotics and Autonomous Systems*, 8 (3) (1991) 203-212.

[11] K. Sathirakul and R. H. Sturges, Jamming conditions for multiple peg-in-hole assemblies, *Robotica*, 16 (03) (1998) 329-345.

[12] Y. Xia, Y. Yin and Z. Chen, , Dynamic analysis for peg-in-hole assembly with contact deformation, *The International Journal of Advanced Manufacturing Technology*, 30 (1-2) (2006) 118-128.

[13] M. A. DiCicco, Force control of heavy lift manipulators for high precision insertion tasks, *Doctoral Dissertation*, Massachusetts Institute of Technology (2005).

[14] S. R. Chhatpar and M. S. Branicky, Search strategies for peg-in-hole assemblies with position uncertainty, Intelligent Robots and Systems, *Proceedings. 2001 IEEE/RSJ International Conference on IEEE*, 3 (2001) 1465-1470.

[15] H. Inoue, *Force feedback in precise assembly tasks*, Artificial Intelligence: An MIT perspective, MIT Press (1979) 219-241.

[16] S. Simunovic, An Information approach to parts mating, *Doctoral Dissertation*, Massachusetts Institute of Technology (1979).

[17] W. S. Newman, Y. Zhao, and Y. H. Pao, Interpretation of force and moment signals for compliant peg-in-hole assembly, *Robotics and Automation, Proceedings 2001 ICRA. IEEE International Conference on IEEE*, 1 (2001) 571-576.

[18] J. MacQueen, Some methods for classification and analysis

of multivariate observations, *Proceedings of the fifth Berkeley symposium on mathematical statistics and probability*, 1 (14) (1967) 281-297.

[19] F. Dietrich, D. Buchholz, F. Wobbe, F. Sowinski, A. Raatz, W. Schumacher and F. M. Wahl, On contact models for assembly tasks: experimental investigation beyond the peg-in-hole problem on the example of force-torque maps, *Intelligent Robots and Systems (IROS), 2010 IEEE/RSJ International Conference on IEEE* (2010) 2313-2323.

[20] H. Chen, J. Wang, G. Zhang, T. Fuhlbrigge and S. Kock, High-precision assembly automation based on robot compliance, *The International Journal of Advanced Manufacturing Technology*, 45 (9-10) (2009) 999-1006.

[21] H. Park, J. H. Bae, J. H. Park, M. H. Baeg and J. Park, Intuitive peg-in-hole assembly strategy with a compliant manipulator, *Robotics (ISR), 2013 44th International Symposium on IEEE* (2013) 1-5.

[22] S. Lee and H. Asada, Assembly of parts with irregular surfaces using active force sensing, *Robotics and Automation, Proceedings, 1994 IEEE International Conference on IEEE* (1994) 2639-2644.

[23] S. Lee and H. Asada, Direct adaptive control of force-guided assembly robots using tuned dither, *American Control Conference, Proceedings of the 1995 IEEE*, 1 (1995) 370-374.

[24] S. Lee and H. H. Asada, A perturbation/correlation method for force guided robot assembly, *Robotics and Automation, IEEE Transactions on*, 15 (4) (1999) 764-773.

[25] B. Bakšys and S. Kilikevičius, Insertion simulation cylindrical parts under kinematical excitation of mobile based part., *Mechanika*, 1 (63) (2007) 38-44.

[26] B. Bakšys and S. Kilikevičius, Experimental investigation of cylindrical parts robotic vibratory insertion, *Mechanika.-Kaunas: Technologija* (2) (2008) 70.

Jaesung Oh received his B.S. degrees in Mechanical and Control Engineering from the Handong Global University, Pohang, South Korea, and his M.S. degree in Mechanical Engineering from the Korea Advanced Institute of Science and Tech-nology (KAIST), Daejeon, South Korea, in 2013 and 2015, respectively. He is currently a graduate student in the Ph.D. course in the Department of Mechanical Engineering, KAIST. His research interests include humanoid robot and applications of robotics and control.

Jun-Ho Oh received his B.S. and M.S. degrees in Mechanical Engineering from Yonsei University, Seoul, South Korea, and his Ph.D. degree in Mechanical Engineering from the University of California, Berkeley, in 1977, 1979, and 1985, respectively. Since 1985, he has been with the Department of Mechanical Engineering, Korea Advanced Institute of Science and Technology (KAIST), where he is currently a Professor and a Director of the Humanoid Robot Research Center. His research interests include humanoid robots, sensors, actuators, and applications of microprocessors. He is a member of the IEEE, KSME, KSPE, and ICROS.